GEOLOGY

E: geology@geosociety.org
W: geosociety.org/gsa
T: @geosociety

FOR PEER REVIEW - CONFIDENTIAL

Delayed sedimentary response to abrupt climate change at the Paleocene-Eocene boundary, northern Spain.

Tracking no: G45631R

Authors:
Robert Duller (University of Liverpool), John Armitage (Institut de Physique du Globe de Paris), Hayley Manners (University of Plymouth), Stephen Grimes (University of Plymouth), and Tom Dunkley -Jones

Abstract:
Sediment routing systems (SRS) are a critical element of the global response to ongoing climate change. However SRS response to climate forcing is complex, fragmentary and obscured when viewed over short, human timescales (10-1-102 yrs). Over long timescales (>102-103 yrs) the aggregated, system-wide response of SRS to climate forcing can be gleaned with more confidence from the sedimentary record; but the nature and timescales of this aggregated response to abrupt climate change is still poorly understood. Here, we investigate the aggregated temporal response of a SRS in northern Spain to abrupt climate warming at the Paleocene-Eocene thermal maximum (PETM). Our results show that terrestrial sites in northern Spain record a temporal lag of 16.5{plus minus}7.5 kyrs between the onset of the PETM, defined by an abrupt negative excursion in δ13C profile, and the onset of coarse-grained deposition. Within the same SRS at the deep marine site 500 km to the west we observe a temporal lag of 16.5{plus minus}1.5 kyrs using an age model independent of that used for the terrestrial sites. These results suggest that the aggregated, system-wide response of SRS to present-day global warming - if we take the PETM as an appropriate modern-day analogue - may persist for many millennia into the future.

DOI:10.1130/G45631.1

Delayed sedimentary response to abrupt climate change at the Paleocene-Eocene boundary, northern Spain.

Robert A. Duller[1], John J. Armitage[2], Hayley Manners[3], Stephen Grimes[3], Tom Dunkley Jones[4]

[1] Department of Earth, Ocean and Ecological Sciences, University of Liverpool, Liverpool L69 3BX, UK

[2]Institut de physique du globe de Paris–Sorbonne Paris Cité, Université Paris Diderot, CNRS, UMR7154, 1 rue Jussieu, 75238 Paris CEDEX 05, France

[3]School of Geography, Earth & Environmental Sciences, Plymouth University, Drake Circus, Plymouth, Devon PL4 8AA, UK

[4]School of Geography, Earth and Environmental Sciences, University of Birmingham, Edgbaston, Birmingham B15 2TT, UK

ABSTRACT

Sediment routing systems (SRSs) are a critical element of the global response to ongoing climate change. However SRS response to climate forcing is complex, fragmentary, and obscured when viewed over short, human time scales (10^{-1}–10^{2} yr). Over long time scales (>10^{2}–10^{3} yr), the aggregated, system-wide response of SRSs to climate forcing can be gleaned with more confidence from the sedimentary record; but the nature and time scales of this aggregated response to abrupt climate change is still poorly understood. Here, we investigate the aggregated temporal response of a SRS in northern Spain to abrupt climate warming at the Paleocene-Eocene thermal maximum (PETM). Our results show that terrestrial sites in northern Spain record a temporal lag of

16.5 ± 7.5 k.y. between the onset of the PETM, defined by an abrupt negative excursion in the $\delta^{13}C$ profile, and the onset of coarse-grained deposition. Within the same SRS at the deep marine site 500 km to the west, we observe a temporal lag of 16.5 ± 1.5 k.y. using an age model that is independent of that used for the terrestrial sites. These results suggest that the aggregated, system-wide response of SRSs to present-day global warming—if we take the PETM as an appropriate modern-day analogue—may persist for many millennia into the future.

INTRODUCTION

The Paleocene-Eocene thermal maximum (PETM) is the most informative geological analogue for understanding the impact of rapid (<5 k.y.) and large-magnitude (>4 °C) warming on global hydrology and sediment routing systems (SRSs) (Haywood et al., 2011; Foreman et al., 2012; Carmichael et al., 2017). The PETM is associated with a large negative carbon isotope excursion (CIE) driven by the release of >4000 Pg of isotopically light carbon into the global carbon cycle (Gutjahr et al. 2017). This event is recorded in the carbon isotope ($\delta^{13}C$) values of calcium carbonate minerals and organic matter from both terrestrial and marine strata (McInerney and Wing, 2011). During the PETM, changes in atmospheric and ocean surface temperature caused dramatic and globally non-uniform change of the hydrological cycle (Bowen and Bowen, 2008; Carmichael et al., 2017). Studies of mid-latitude areas in the central United States (Foreman et al. 2012; Kraus et al., 2013; Baczynski et al., 2013) and northern Spain (Schmitz and Pujalte 2007; Manners et al., 2013) indicate increased seasonal precipitation during the PETM, within generally dry climate regimes. In northern Spain, there is a clear association between the CIE and an increase in the amount, and caliber, of detrital material transported to both terrestrial and marine environments (Schmitz and Pujalte, 2003, 2007; Dunkley Jones et al. 2018; Pujalte et al. 2015). A laterally extensive (>500 km^2), 1–7-m-thick conglomerate unit ('Claret Conglomerate') marks this change in the terrestrial environment (Schmitz and Pujalte, 2003). Similarly, in Wyoming, USA, a 30-m-thick and laterally extensive channel-belt sandstone ('Boundary Sandstone') is concomitant with the PETM (Foreman, 2014); and in Colorado, a similar change in sedimentary architecture is associated with the PETM (Foreman et al., 2012). The short temporal duration of PETM onset (<5 k.y.) (Bowen et al., 2015; Dunkley Jones et al. 2018) and the potential for precise, high-resolution stratigraphic correlation between sections using $\delta^{13}C$ data, enables PETM Earth system leads and lags to be resolved at the millennial scale (Knight and Harrison, 2013). The preservation and exposure of terrestrial and deep-marine PETM sequences in the Tremp-Graus Basin of northern Spain (Schmitz and Pujalte, 2003, 2007; Domingo et al., 2009; Manners et al., 2013; Dunkley Jones et al., 2018) allows the study of system-wide response of a SRS to rapid and abrupt climate warming. We use these sequences in northern Spain to explore the aggregated, system-wide response of a PETM SRS.

METHODS

To quantify the temporal relationship between the onset of the PETM climate perturbation and the response of the Spanish PETM SRS, we first assume a close coupling existed between the onset character of the CIE and PETM climate. This is supported by high-resolution studies of expanded PETM sections from the New Jersey margin that find no significant lag between $\delta^{13}C$ and $\delta^{18}O$ records (Zeebe et al. 2016). Here we focus on quantifying the lag time (t_{lag}) between the onset of the CIE and the onset of coarse-grained detrital deposition (OCD) in a study section. To do this, we first calculate a mean sedimentation rate for each section using the latest estimates of PETM CIE duration (Westerhold et al. 2018) and the measured stratigraphic thickness of the CIE at each location. To account for uncertainty in the precise identification of the CIE "core" (ca. 100 ka) versus "core and recovery" (ca. 180 ka) in the study sections, we calculate lower and upper estimates for sedimentation rate using both these durations (Westerhold et al., 2018).

Our approach should give a minimum t_{lag} values for two reasons. First, sedimentation rates in most sections increase substantially during the core of the PETM (Dunkley Jones et al., 2018; John et al., 2007), and applying these higher sedimentation rate values to the onset phase will minimize calculated t_{lag} values. Second, the basal surface of the Claret Conglomerate in the Spanish Sections remove and truncate underlying strata that accumulated during the onset interval of the PETM. Therefore, the preservation of a stratigraphic offset between the onset of the PETM CIE and the base of the Claret Conglomerate is strong evidence for a temporal lag of SRS response. On this basis, the t_{lag} values calculated here are almost certainly minimum estimates. We note that, for our purposes, the calculation of t_{lag} is not compromised by the 'Sadler effect' (Sadler, 1981).

To further explore the stratigraphic response of SRSs to abrupt hydrological change, we utilize a one-dimensional (1-D) sediment transport model (see the GSA Data Repository[1]). The model solves for the change in topography due to the transport of sediment down slope, which is a function of both local slope and surface water discharge (Armitage et al., 2016). Precipitation rate is increased from a baseline of 0.5 mm yr^{-1}

following a box profile with a time to peak precipitation of 5 k.y. reflecting the time scale of PETM onset (Westerhold et al., 2018).

RESULTS

The analysis shows that the Tendrui, Claret, and Campo sections exhibit a stratigraphic offset, but that the Esplugafreda section does not (Fig. 2). The calculated durations of the stratigraphic offset or t_{lag} are: Tendrui t_{lag} = 13–24 k.y.; Claret t_{lag} = 9–16 k.y.; Esplugafreda t_{lag} = 0 k.y. The lower rates of sediment accumulation at the Esplugafreda section (0.1 mm yr^{-1}) has led to a reduced level of stratigraphic completeness (Sadler, 1981; Straub and Esposito, 2013); inhibiting proxy record preservation and precluding the identification of a resolvable t_{lag} (Foreman and Straub, 2017). We tentatively estimate a value of Campo t_{lag} = 20–36 k.y.

A new age model for the deep marine segment of this SRS at Zumaia (Fig. 1), alongside a record of detrital mass accumulation rate (D_{MAR}) (Dunkley Jones et al., 2018), allows for a unique comparison of the terrestrial and marine response to the same event. The D_{MAR} data from the Zumaia section shows an immediate response to the CIE, increasing from 1 g cm^{-2} $k.y.^{-1}$ to 3 g cm^{-2} $k.y.^{-1}$ over the first 5 k.y. (Fig. 2E). This elevated value is maintained for 10 k.y. before increasing abruptly from 3 g cm^{-2} $k.y.^{-1}$ to 7 g cm^{-2} $k.y.^{-1}$ over a period of <4 k.y., an increase that lags behind the CIE by t_{lag} = 15–18 k.y.; while maximum D_{MAR} values are attained 25–30 k.y. after the onset of the CIE (Fig. 2E). The immediate response of D_{MAR} to the CIE is due to the greater advective length scales or transportability of finer-grained material (Ganti et al., 2014). However, the synchroneity of the arrival of coarse material at the terrestrial sites and the increase in D_{MAR} at the deep marine site suggests that a single causative mechanism is responsible for the observed time lag. The data presented above strongly suggest that SRSs may take ~10^4 yrs to respond to abrupt, large magnitude climate change.

The results of the 1-D sediment transport model demonstrate that a t_{lag} can be reproduced (Fig. 3). The greater the precipitation increase over the 5 k.y. onset duration, the shorter the value of t_{lag} (Fig. 3). The truncation of individual grain size profiles (e.g., Fig. 3B) signifies sediment bypass and non-deposition (i.e. a time gap) of the coarsest grain size populations. In northern Spain we suggest that this phase of by-pass is recorded as a 20–30-m-thick succession of fine-grained floodplain sediment that directly overlies the Claret Conglomerate. The model predicts t_{lag} values of 0 k.y. at 50 km distance from the origin, 10–35 k.y. at 100 km, and 45–85 k.y. at 150 km (Fig. 3D), which is not dissimilar to the field estimates of t_{lag}. We acknowledge that these model results are approximations.

DISCUSSION

Stratigraphic sections from the terrestrial and deep marine segments of the northern Spain PETM SRS show strong evidence for a time lag between the onset of the PETM CIE and the onset of coarse-grained deposition. The results of a 1-D sediment transport model support this. The observed t_{lag} was generated by the internal response of the SRS; so what was this mechanism? It is possible that the natural avulsion of river channels could generate a stratigraphic offset and so t_{lag}, but the t_{lag} value would be spatially variable. This maximum value of an *avulsion-related time lag* can be approximated by a compensation timescale, $T_c = h/r$, (where h is channel depth and r is aggradation rate). This defines the time window over which sediment can be delivered to the majority of a river valley width (Straub et al., 2009; Wang et al., 2011), which is calculated to be T_c = 6.5 ± 3.7 k.y. for the sections in northern Spain. This value of T_c represents a maximum value given that the time taken for a channel to visit 95% of the river valley width could be of the order of ~0.25T_c (Straub and Esposito, 2013), and channel mobility increases with increasing sediment flux (Wickert et al., 2013) and a change in vegetation type and coverage (Foreman, 2014). We note that T_c = 6.5 ± 3.7 k.y. also represents a minimum resolvable lag time using geochemical proxies (Foreman and Straub, 2017). Our preferred mechanism for the generation of t_{lag} is a delay in sediment transport from source area(s) to down-system locations as transport slopes adjust to the increased transport capacity of the fluvial system. This mechanism can explain a SRS-wide response. However, given our limited knowledge of the relationship between temperature change magnitude, the onset of hydrological system response, and the onset of landscape response, we cannot completely rule out a 'critical hydrological-landscape threshold' mechanism, whereby the time it takes to reach this critical threshold is manifested as a t_{lag}. This requires further work.

As a comparison, t_{lag} values were calculated for two well-studied sections in the Piceance Creek basin of western Colorado (Foreman et al., 2012), and the Bighorn Basin of Wyoming (Foreman, 2014), giving values of t_{lag} = 22–40 k.y. and 14–25 k.y., respectively (see the Data Repository). The presence of a t_{lag} in PETM sections in the United States and in northern Spain sections might suggest a common mechanism of generation. However, we advise slight caution on this as the value of t_{lag} will depend on the input grain size of the sediment supply, location within the basin, and local basin and Earth surface conditions that dictate the degree of stratigraphic completeness (Foreman and Straub, 2017).

Given the lag times present in many of the studied PETM sections our results suggest that it may take ≤15 k.y. for SRS to achieve total and aggregated, system-wide response to modern abrupt climate forcing. This time scale probably represents an upper estimate given that anthropogenic carbon release rates are an order of magnitude greater than that associated with the PETM CIE (Zeebe et al., 2016). The aggregated, system-wide response time scale described here is akin to the timescale necessary for 'system clearing' (Jerolmack and Paola, 2010; Foreman et al., 2012) to occur in an individual SRS following abrupt climate forcing. This temporal and spatial character of SRS response is a function of the nature of climate forcing and the size and sensitivity of the SRS (Jerolmack and Paola, 2010; Knight and Harrison, 2013). From a stratigraphic perspective, accurately decoding past climate from sedimentary caliber or type alone is problematic given the observed complex response of SRSs, where sedimentary layers may well be recording an event that took place 10^4 yrs earlier. From the perspective of modern global change, it is clear that the response of SRS to anthropogenically induced climate change has only just started. Based on the available PETM data, dramatic changes in sediment erosion, sediment flux and sediment accumulation rates, across both terrestrial and marine segments of SRS, are likely to evolve and persist for millennia to come.

CONCLUSION

A linked terrestrial to deep marine sediment routing system in northern Spain records a stratigraphic offset between the abrupt onset of warming and hydrological change at the PETM, and the arrival of coarse-grained (>2 mm) material to terrestrial sections, and the increase in detrital mass accumulation rate at a deep marine section. The calculated duration of this stratigraphic offset (t_{lag}) is of the order of 16.5 ± 7.5 k.y. for terrestrial sites and 16.5 ± 1.5 k.y. for the deep-marine site, each using independent age model. This SRS-wide response and t_{lag} value range is reproduced using a 1-D sediment transport model, which supports the mechanism of delayed sediment transport from the sediment source area to locations down-system. Our data provide new field and modeling constraints on the response of SRSs to abrupt climate change and highlight the protracted response of our landscape to current global warming, which may take millennia.

ACKNOWLEDGMENTS

We thank two anonymous reviewers and the editor. Armitage acknowledges funding through the French Agence National de la Recherche, Accueil de Chercheurs de Haut Niveau call, grant “InterRift”.

REFERENCES CITED

Armitage, J.J., Burgess, P.M., Hampson, G.J., and Allen, P.A., 2016, Deciphering the origin of cyclical gravel front and shoreline progradation and retrogradation in the stratigraphic record: Basin Research, v. 30, p. 15–35, https://doi.org/10.1111/bre.12203.

Baczynski, A.A., McInerney, F.A., Wing, S.L., Kraus, M.J., Bloch, J.I., Boyer, D.M., Secord, R., Morse, P.E., and Fricke, H.C., 2013, Chemostratigraphic implications of spatial variation in the Paleocene-Eocene Thermal Maximum carbon isotope excursión, SE Bighorn Basin, Wyoming: Geochemistry Geophysics Geosystems, v. 14, p. 4133–4152, https://doi.org/10.1002/ggge.20265.

Bowen, G.J., and Bowen, B.B., 2008, Mechanisms of PETM global change constrained by a new record from central Utah: Geology, v. 36, p. 379–382, https://doi.org/10.1130/G24597A.1.

Bowen, G.H., Maibauer, B.J., Kraus, M.J., Röhl, U., Westerhold, T., Steimke, A., Gingerich, P.D., Wing, S.L., and Clyde, W.C., 2015, Two massive, rapid releases of carbon during the onset of the Paleocene-Eocene thermal maximum: Nature Geoscience, v. 8, p. 44–47, https://doi.org/10.1038/ngeo2316.

Carmichael, M.J., et al., 2017, Hydrological and associated biogeochemical consequences of rapid global warming during the Paleocene-Eocene Thermal Maximum: Global and Planetary Change, v. 157, p. 114–138, https://doi.org/10.1016/j.gloplacha.2017.07.014.

Domingo, L., López-Martínez, N., Leng, M.J., and Grimes, S.T., 2009, The Paleocene–Eocene Thermal Maximum record in the organic matter of the Claret and Tendruy continental sections (South-central Pyrenees, Lleida, Spain): Earth and Planetary Science Letters, v. 281, p. 226–237, https://doi.org/10.1016/j.epsl.2009.02.025.

Dunkley Jones, T., et al., 2018, Orbital forcing of terrestrial hydrology, weathering and carbon sequestration during the Paleocene-Eocene Thermal Maximum: Climate of the Past, https://doi.org/10.5194/cp-2017-131.

Foreman, B.Z., Heller, P.L., and Clementz, M.T., 2012, Fluvial response to abrupt global warming at the Paleocene/Eocene boundary: Nature, v. 491, p. 92–95, https://doi.org/10.1038/nature11513.

Foreman, B.Z., 2014, Climate-driven generation of a fluvial sheet sand body at the Paleocene-Eocene boundary in north-west Wyoming (USA): Basin Research, v. 26, p. 225–241, https://doi.org/10.1111/bre.12027.

Foreman, B.Z., and Straub, K.M., 2017, Autogenic geomorphic processes determine the resolution and fidelity of terrestrial paleoclimate records: Science Advances, v. 3, p. e1700683, https://doi.org/10.1126/sciadv.1700683.

Ganti, V., Lamb, M.P., and McElroy, B., 2014, Quantitative bounds on morphodynamics and implications for reading the sedimentary record: Nature Communications, v. 5, p. 3298, https://doi.org/10.1038/ncomms4298.

Gutjahr, M., Ridgwell, A., Sexton, P.F., Anagnostou, E., Pearson, P.N., Pälike, H., Norris, R.D., Thomas, E., and Foster, G.L., 2017, Very large release of mostly volcanic carbon during the Palaeocene–Eocene Thermal Maximum: Nature, v. 548, p. 573–577, https://doi.org/10.1038/nature23646.

Haywood, A.M., Ridgwell, A., Lunt, D.J., Hill, D.J., Pound, M.J., Dowsett, H.J., Dolan, A.M., Francis, J.E., and Williams, M., 2011, Are there pre-Quaternary geological analogues for a future greenhouse warming?: Philosophical Transactions of the Royal Society, v. 369, p. 933–956, https://doi.org/10.1098/rsta.2010.0317.

Jerolmack, D.J., and Paola, C., 2010, Shredding of environmental signals by sediment transport: Geophysical Research Letters, v. 37, L19401, https://doi.org/10.1029/2010GL044638.

John, C.M., Bohaty, S.N., Zachos, J.C., Sluijs, A., Gibbs, S., Brinkhuis, H., and Bralower, T.J., 2007, North American continental margin records of the Paleocene-

Eocene thermal maximum: Implications for global carbon and hydrological cycling: Paleoceanography, v. 23, PA2217, https://doi.org/10.1029/2007PA001465.

Knight, J., and Harrison, S., 2013, The impacts of climate change on terrestrial Earth surface systems: Nature Climate Change, v. 3, p. 24–29, https://doi.org/10.1038/nclimate1660.

Kraus, M.J., McInerney, F.A., Wing, S.L., Secord, R., Baczynski, A.A., and Bloch, J.I., 2013, Paleohydrologic response to continental warming during the Paleocene-Eocene Thermal Maximum, Bighorn Basin, Wyoming: Palaeogeography, Palaeoclimatology, Palaeoecology, v. 370, p. 196–208, https://doi.org/10.1016/j.palaeo.2012.12.008.

Manners, H.R., et al., 2013, Magnitude and profile of organic carbon isotope records from the Paleocene-Eocene Thermal Maximum: evidence from northern Spain: Earth and Planetary Science Letters, v. 376, p. 220–230, https://doi.org/10.1016/j.epsl.2013.06.016.

McInerney, F.A., and Wing, S.L., 2011, The paleocene-eocene thermal maximum: A perturbation of carbon cycle, climate, and biosphere with implications for the future: Annual Review of Earth and Planetary Sciences, v. 39, p. 489–516, https://doi.org/10.1146/annurev-earth-040610-133431.

Pujalte, V., Baceta, J.I., and Schmitz, B., 2015, A massive input of coarse-grained siliciclastics in the Pyrenean Basin during the PETM: The missing ingredient in a coeval abrupt change in hydrological regime: Climate of the Past, v. 11, p. 1653–1672, https://doi.org/10.5194/cp-11-1653-2015.

Sadler, P.M., 1981, Sediment accumulation rates and the completeness of stratigraphic sections: The Journal of Geology, v. 89, p. 569–584, https://doi.org/10.1086/628623.

Schmitz, B., and Pujalte, V., 2003, Sea-level, humidity, and land-erosion records across the initial Eocene thermal maximum from a continental-marine transect in northern Spain: Geology, v. 31, p. 689–692, https://doi.org/10.1130/G19527.1.

Schmitz, B., and Pujalte, V., 2007, Abrupt increase in seasonal extreme precipitation at the Paleocene-Eocene boundary: Geology, v. 35, p. 215–218, https://doi.org/10.1130/G23261A.1.

Straub, K.M., Paola, C., Mohrig, D., Wolinsky, M.A., and George, T., 2009, Compensational stacking of channelized sedimentary deposits: Journal of Sedimentary Research, v. 79, p. 673–688, https://doi.org/10.2110/jsr.2009.070.

Straub, K.M., and Esposito, C.R., 2013, Influence of water and sediment supply on the stratigraphic record of alluvial fans and deltas: Process controls on stratigraphic completeness: Journal of Geophysical Research: Earth Surface, v. 118, p. 625–637, https://doi.org/10.1002/jgrf.20061.

Wang, Y., Straub, K.M., and Hajek, E.A., 2011, Scale-dependent compensational stacking: An estimate of autogenic time scales in channelized sedimentary deposits: Geology, v. 39, p. 811–814, https://doi.org/10.1130/G32068.1.

Westerhold, T., Röhl, U., Wilkens, R., Gingerich, P.D., Clyde, W., Wing, S., Bowen, G., and Kraus, M., 2018, Synchronizing early Eocene deep-sea and continental records—New cyclostratigraphic age models from the Bighorn Basin Coring Project: Climate of the Past, v. 14, p. 303–319, https://doi.org/10.5194/cp-14-303-2018.

Wickert, A.D., Martin, J.M., Tal, M., Kim, W., Sheets, B., and Paola, C., 2013, River channel lateral mobility: metrics, time scales, and controls: Journal of Geophysical Research: Earth Surface, v. 118, p. 396–412, https://doi.org/10.1029/2012JF002386.

Zeebe, R.E., Ridgwell, A., and Zachos, J.C., 2016, Anthropogenic carbon release rate unprecedented during the past 66 million years: Nature Geoscience, v. 9, p. 325–329, https://doi.org/10.1038/ngeo2681.

FIGURE CAPTIONS

Figure 1. Site location, location map, and early Paleogene paleogeography of the Spanish Pyrenees. Section locations: CL—Claret; T—Tendrui; E—Esplugafreda; C—Campo; Z—Zumaia. Main cities: Sa—Santander; SS—San Sebastian; Vi—Vitoria; To—Toulouse. Modified from Pujalte et al. (2015).

Figure 2. Sedimentary logs and associated isotopic profiles. Sections in northern Spain are: A—Tendrui; B—Claret; C—Esplugafreda D—Campo (Manners et al., 2013); E—Zumaia (Dunkley Jones et al., 2018). Dark gray solid line overlaying carbon isotope data in A, B, and C represents the five-point running average of the data.

Figure 3. Model results of time delay as a function of distance from source. A: Four ‘increased precipitation’ scenarios, each with an initial starting value of 0.5 m yr^{-1}. B, C: Chronostratigraphic plots showing the grain size response of each precipitation scenario. PO—PETM onset; OCD—onset of coarse detrital deposition; SBP—sediment by-pass. The time difference between PO and OCD is the time delay or lag (t_{lag}). D: Model t_{lag} results (white fill symbols) and field data results (greyscale filled symbols) plotted as a

function of distance. T—Tendrui; CL—Claret; C—Campo; Z—Zumaia; D_{MAR} max—Maximum detrital mass accumulation rate at Zumaia (Dunkley Jones et al., 2018).

[1]GSA Data Repository item 2019xxx, details of 1-D sediment transport model and values used to calculate the duration of stratigraphic offset, is available online at www.geosociety.org/pubs/ft2019.htm, or on request from editing@geosociety.org.

Figure 1

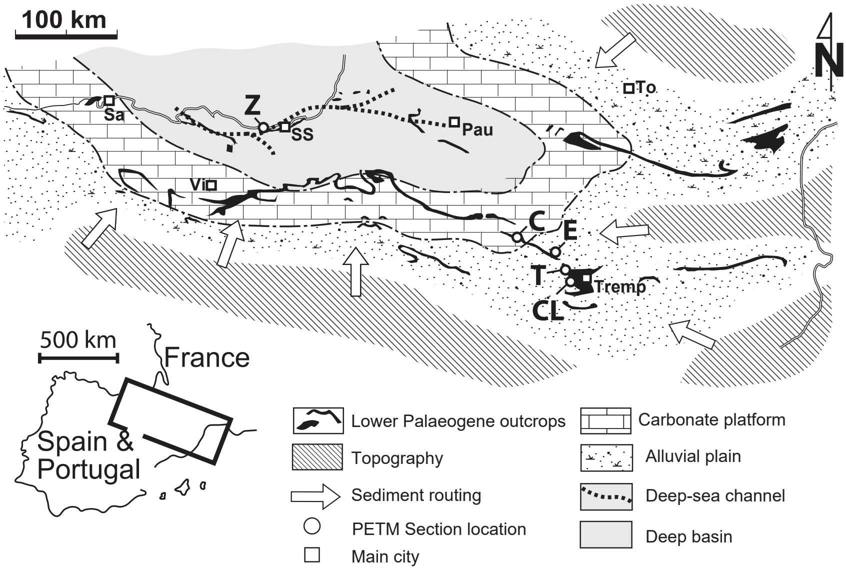

100 km
N
Z
Sa
SS
Pau
To
Vi
C
E
T
Tremp
CL
500 km
France
Spain &
Portugal
Lower Palaeogene outcrops
Topography
Sediment routing
PETM Section location
Main city
Carbonate platform
Alluvial plain
Deep-sea channel
Deep basin

Figure 2

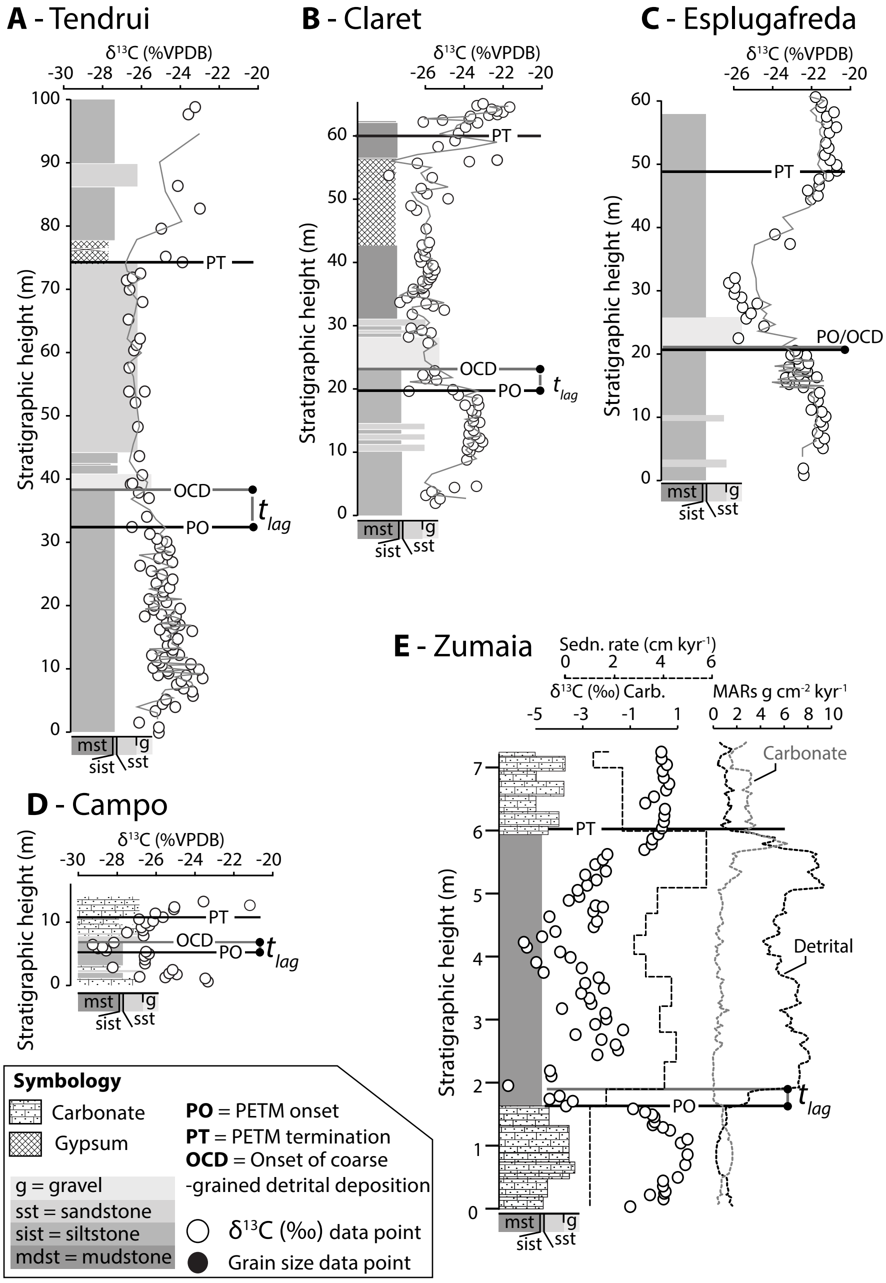

A - Tendrui
B - Claret
C - Esplugafreda
D - Campo
E - Zumaia
δ13C (%VPDB)
Stratigraphic height (m)
PT
OCD
PO
PO/OCD
t lag
mst
sist
sst
g
Sedn. rate (cm kyr-1)
δ13C (‰) Carb.
MARs g cm-2 kyr-1
Carbonate
Detrital
Symbology
Carbonate
Gypsum
PO = PETM onset
PT = PETM termination
OCD = Onset of coarse -grained detrital deposition
g = gravel
sst = sandstone
sist = siltstone
mdst = mudstone
δ13C (‰) data point
Grain size data point

Figure 3

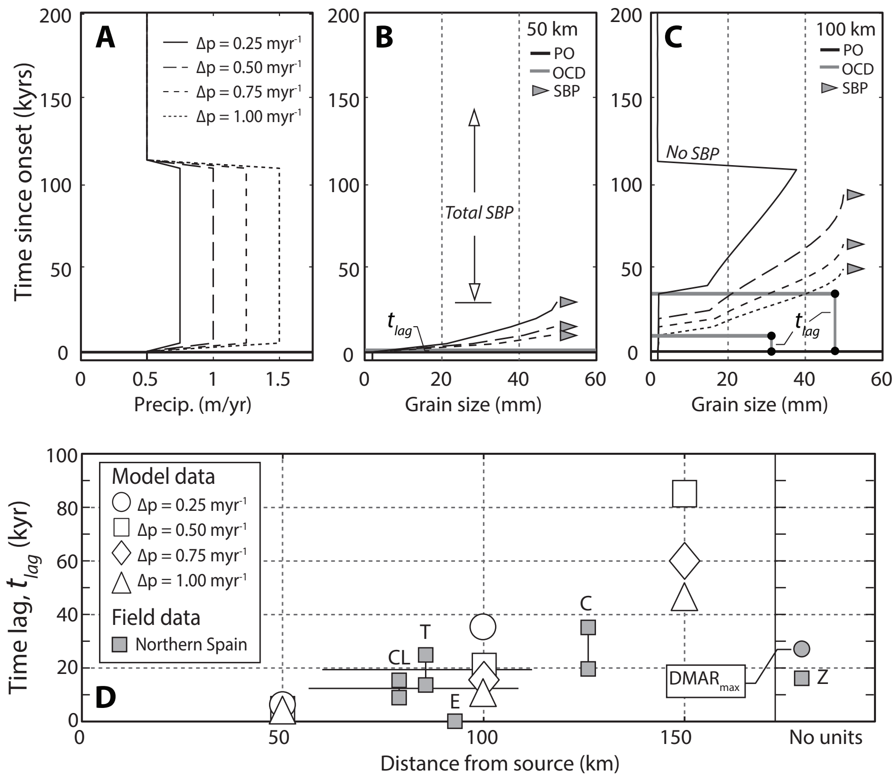

A
Δp = 0.25 myr⁻¹
Δp = 0.50 myr⁻¹
Δp = 0.75 myr⁻¹
Δp = 1.00 myr⁻¹
Time since onset (kyrs)
Precip. (m/yr)
B
50 km
PO
OCD
SBP
Total SBP
t lag
Grain size (mm)
C
100 km
PO
OCD
SBP
No SBP
t lag
Grain size (mm)
D
Model data
Δp = 0.25 myr⁻¹
Δp = 0.50 myr⁻¹
Δp = 0.75 myr⁻¹
Δp = 1.00 myr⁻¹
Field data
Northern Spain
Time lag, t lag (kyr)
T
CL
E
C
DMAR max
Z
Distance from source (km)
No units